EUROPEAN LABORATORY FOR PARTICLE PHYSICS

CERN-EP/98-114
July 16, 1998

A Study of Parton Fragmentation in Hadronic Z^0 Decays Using $\Lambda\bar{\Lambda}$ Correlations

The OPAL Collaboration

Abstract

The correlated production of Λ and $\bar{\Lambda}$ baryons has been studied using 4.3 million multihadronic Z^0 decays recorded with the OPAL detector at LEP. Di-lambda pairs were investigated in the full data sample and for the first time also in 2-jet and 3-jet events selected with the $k_\perp$ algorithm. The distributions of rapidity differences from correlated $\Lambda\bar{\Lambda}$ pairs exhibit short-range, local correlations and prove to be a sensitive tool to test models, particularly for 2-jet events. The JETSET model describes the data best but some extra parameter tuning is needed to improve agreement with the experimental results in the rates and the rapidity spectra simultaneously. The recently developed modification of JETSET, the MOdified Popcorn Scenarium (MOPS), and also HERWIG do not give satisfactory results. This study of di-lambda production in 2- and 3-jet events supports the short-range compensation of quantum numbers.

(Submitted to Physics Letters B)

The OPAL Collaboration

G. Abbiendi[2], K. Ackerstaff[8], G. Alexander[23], J. Allison[16], N. Altekamp[5], K.J. Anderson[9], S. Anderson[12], S. Arcelli[17], S. Asai[24], S.F. Ashby[1], D. Axen[29], G. Azuelos[18,a], A.H. Ball[17], E. Barberio[8], R.J. Barlow[16], R. Bartoldus[3], J.R. Batley[5], S. Baumann[3], J. Bechtluft[14], T. Behnke[27], K.W. Bell[20], G. Bella[23], A. Bellerive[9], S. Bentvelsen[8], S. Bethke[14], S. Betts[15], O. Biebel[14], A. Biguzzi[5], S.D. Bird[16], V. Blobel[27], I.J. Bloodworth[1], M. Bobinski[10], P. Bock[11], J. Böhme[14], D. Bonacorsi[2], M. Boutemeur[34], S. Braibant[8], P. Bright-Thomas[1], L. Brigliadori[2], R.M. Brown[20], H.J. Burckhart[8], C. Burgard[8], R. Bürgin[10], P. Capiluppi[2], R.K. Carnegie[6], A.A. Carter[13], J.R. Carter[5], C.Y. Chang[17], D.G. Charlton[1,b], D. Chrisman[4], C. Ciocca[2], P.E.L. Clarke[15], E. Clay[15], I. Cohen[23], J.E. Conboy[15], O.C. Cooke[8], C. Couyoumtzelis[13], R.L. Coxe[9], M. Cuffiani[2], S. Dado[22], G.M. Dallavalle[2], R. Davis[30], S. De Jong[12], L.A. del Pozo[4], A. de Roeck[8], K. Desch[8], B. Dienes[33,d], M.S. Dixit[7], J. Dubbert[34], E. Duchovni[26], G. Duckeck[34], I.P. Duerdoth[16], D. Eatough[16], P.G. Estabrooks[6], E. Etzion[23], H.G. Evans[9], F. Fabbri[2], M. Fanti[2], A.A. Faust[30], F. Fiedler[27], M. Fierro[2], I. Fleck[8], R. Folman[26], A. Fürtjes[8], D.I. Futyan[16], P. Gagnon[7], J.W. Gary[4], J. Gascon[18], S.M. Gascon-Shotkin[17], G. Gaycken[27], C. Geich-Gimbel[3], G. Giacomelli[2], P. Giacomelli[2], V. Gibson[5], W.R. Gibson[13], D.M. Gingrich[30,a], D. Glenzinski[9], J. Goldberg[22], W. Gorn[4], C. Grandi[2], E. Gross[26], J. Grunhaus[23], M. Gruwé[27], G.G. Hanson[12], M. Hansroul[8], M. Hapke[13], K. Harder[27], C.K. Hargrove[7], C. Hartmann[3], M. Hauschild[8], C.M. Hawkes[5], R. Hawkings[27], R.J. Hemingway[6], M. Herndon[17], G. Herten[10], R.D. Heuer[8], M.D. Hildreth[8], J.C. Hill[5], S.J. Hillier[1], P.R. Hobson[25], A. Hocker[9], R.J. Homer[1], A.K. Honma[28,a], D. Horváth[32,c], K.R. Hossain[30], R. Howard[29], P. Hüntemeyer[27], P. Igo-Kemenes[11], D.C. Imrie[25], K. Ishii[24], F.R. Jacob[20], A. Jawahery[17], H. Jeremie[18], M. Jimack[1], C.R. Jones[5], P. Jovanovic[1], T.R. Junk[6], D. Karlen[6], V. Kartvelishvili[16], K. Kawagoe[24], T. Kawamoto[24], P.I. Kayal[30], R.K. Keeler[28], R.G. Kellogg[17], B.W. Kennedy[20], A. Klier[26], S. Kluth[8], T. Kobayashi[24], M. Kobel[3,e], D.S. Koetke[6], T.P. Kokott[3], M. Kolrep[10], S. Komamiya[24], R.V. Kowalewski[28], T. Kress[11], P. Krieger[6], J. von Krogh[11], T. Kuhl[3], P. Kyberd[13], G.D. Lafferty[16], D. Lanske[14], J. Lauber[15], S.R. Lautenschlager[31], I. Lawson[28], J.G. Layter[4], D. Lazic[22], A.M. Lee[31], D. Lellouch[26], J. Letts[12], L. Levinson[26], R. Liebisch[11], B. List[8], C. Littlewood[5], A.W. Lloyd[1], S.L. Lloyd[13], F.K. Loebinger[16], G.D. Long[28], M.J. Losty[7], J. Ludwig[10], D. Liu[12], A. Macchiolo[2], A. Macpherson[30], W. Mader[3], M. Mannelli[8], S. Marcellini[2], C. Markopoulos[13], A.J. Martin[13], J.P. Martin[18], G. Martinez[17], T. Mashimo[24], P. Mättig[26], W.J. McDonald[30], J. McKenna[29], E.A. Mckigney[15], T.J. McMahon[1], R.A. McPherson[28], F. Meijers[8], S. Menke[3], F.S. Merritt[9], H. Mes[7], J. Meyer[27], A. Michelini[2], S. Mihara[24], G. Mikenberg[26], D.J. Miller[15], R. Mir[26], W. Mohr[10], A. Montanari[2], T. Mori[24], K. Nagai[8], I. Nakamura[24], H.A. Neal[12], B. Nellen[3], R. Nisius[8], S.W. O'Neale[1], F.G. Oakham[7], F. Odorici[2], H.O. Ogren[12], M.J. Oreglia[9], S. Orito[24], J. Pálinkás[33,d], G. Pásztor[32], J.R. Pater[16], G.N. Patrick[20], J. Patt[10], R. Perez-Ochoa[8], S. Petzold[27], P. Pfeifenschneider[14], J.E. Pilcher[9], J. Pinfold[30], D.E. Plane[8], P. Poffenberger[28], J. Polok[8], M. Przybycień[8], C. Rembser[8], H. Rick[8], S. Robertson[28], S.A. Robins[22], N. Rodning[30], J.M. Roney[28], K. Roscoe[16], A.M. Rossi[2], Y. Rozen[22], K. Runge[10], O. Runolfsson[8], D.R. Rust[12], K. Sachs[10], T. Saeki[24], O. Sahr[34], W.M. Sang[25], E.K.G. Sarkisyan[23], C. Sbarra[29], A.D. Schaile[34], O. Schaile[34], F. Scharf[3], P. Scharff-Hansen[8], J. Schieck[11], B. Schmitt[8], S. Schmitt[11], R.E. Schmitz[3], A. Schöning[8], M. Schröder[8], M. Schumacher[3], C. Schwick[8], W.G. Scott[20], R. Seuster[14], T.G. Shears[8], B.C. Shen[4], C.H. Shepherd-Themistocleous[8], P. Sherwood[15], G.P. Siroli[2], A. Sittler[27], A. Skuja[17], A.M. Smith[8], G.A. Snow[17], R. Sobie[28],

S. Söldner-Rembold[10], M. Sproston[20], A. Stahl[3], K. Stephens[16], J. Steuerer[27], K. Stoll[10], D. Strom[19], R. Ströhmer[34], B. Surrow[8], S.D. Talbot[1], S. Tanaka[24], P. Taras[18], S. Tarem[22], R. Teuscher[8], M. Thiergen[10], M.A. Thomson[8], E. von Törne[3], E. Torrence[8], S. Towers[6], I. Trigger[18], Z. Trócsányi[33], E. Tsur[23], A.S. Turcot[9], M.F. Turner-Watson[8], R. Van Kooten[12], P. Vannerem[10], M. Verzocchi[10], H. Voss[3], F. Wäckerle[10], A. Wagner[27], C.P. Ward[5], D.R. Ward[5], P.M. Watkins[1], A.T. Watson[1], N.K. Watson[1], P.S. Wells[8], N. Wermes[3], J.S. White[6], G.W. Wilson[16], J.A. Wilson[1], T.R. Wyatt[16], S. Yamashita[24], G. Yekutieli[26], V. Zacek[18], D. Zer-Zion[8]

[1]School of Physics and Astronomy, University of Birmingham, Birmingham B15 2TT, UK
[2]Dipartimento di Fisica dell' Università di Bologna and INFN, I-40126 Bologna, Italy
[3]Physikalisches Institut, Universität Bonn, D-53115 Bonn, Germany
[4]Department of Physics, University of California, Riverside CA 92521, USA
[5]Cavendish Laboratory, Cambridge CB3 0HE, UK
[6]Ottawa-Carleton Institute for Physics, Department of Physics, Carleton University, Ottawa, Ontario K1S 5B6, Canada
[7]Centre for Research in Particle Physics, Carleton University, Ottawa, Ontario K1S 5B6, Canada
[8]CERN, European Organisation for Particle Physics, CH-1211 Geneva 23, Switzerland
[9]Enrico Fermi Institute and Department of Physics, University of Chicago, Chicago IL 60637, USA
[10]Fakultät für Physik, Albert Ludwigs Universität, D-79104 Freiburg, Germany
[11]Physikalisches Institut, Universität Heidelberg, D-69120 Heidelberg, Germany
[12]Indiana University, Department of Physics, Swain Hall West 117, Bloomington IN 47405, USA
[13]Queen Mary and Westfield College, University of London, London E1 4NS, UK
[14]Technische Hochschule Aachen, III Physikalisches Institut, Sommerfeldstrasse 26-28, D-52056 Aachen, Germany
[15]University College London, London WC1E 6BT, UK
[16]Department of Physics, Schuster Laboratory, The University, Manchester M13 9PL, UK
[17]Department of Physics, University of Maryland, College Park, MD 20742, USA
[18]Laboratoire de Physique Nucléaire, Université de Montréal, Montréal, Quebec H3C 3J7, Canada
[19]University of Oregon, Department of Physics, Eugene OR 97403, USA
[20]CLRC Rutherford Appleton Laboratory, Chilton, Didcot, Oxfordshire OX11 0QX, UK
[22]Department of Physics, Technion-Israel Institute of Technology, Haifa 32000, Israel
[23]Department of Physics and Astronomy, Tel Aviv University, Tel Aviv 69978, Israel
[24]International Centre for Elementary Particle Physics and Department of Physics, University of Tokyo, Tokyo 113, and Kobe University, Kobe 657, Japan
[25]Institute of Physical and Environmental Sciences, Brunel University, Uxbridge, Middlesex UB8 3PH, UK
[26]Particle Physics Department, Weizmann Institute of Science, Rehovot 76100, Israel
[27]Universität Hamburg/DESY, II Institut für Experimental Physik, Notkestrasse 85, D-22607 Hamburg, Germany
[28]University of Victoria, Department of Physics, P O Box 3055, Victoria BC V8W 3P6, Canada
[29]University of British Columbia, Department of Physics, Vancouver BC V6T 1Z1, Canada

[30]University of Alberta, Department of Physics, Edmonton AB T6G 2J1, Canada
[31]Duke University, Dept of Physics, Durham, NC 27708-0305, USA
[32]Research Institute for Particle and Nuclear Physics, H-1525 Budapest, P O Box 49, Hungary
[33]Institute of Nuclear Research, H-4001 Debrecen, P O Box 51, Hungary
[34]Ludwigs-Maximilians-Universität München, Sektion Physik, Am Coulombwall 1, D-85748 Garching, Germany

[a] and at TRIUMF, Vancouver, Canada V6T 2A3
[b] and Royal Society University Research Fellow
[c] and Institute of Nuclear Research, Debrecen, Hungary
[d] and Department of Experimental Physics, Lajos Kossuth University, Debrecen, Hungary
[e] on leave of absence from the University of Freiburg

1 Introduction

The compensation of quantum numbers plays a key role in our understanding of the fragmentation process whereby partons transform into observable hadrons. Consequently, baryon production in hadronic e^+e^- annihilation final states provides data very well suited to test phenomenological fragmentation models. In particular, the study of di-lambda pairs allows a subtle testing of model predictions because of the relatively large rates and the necessity to compensate two quantum numbers: baryon number and strangeness.

Fragmentation models such as JETSET [1] and HERWIG [2] are based on a chainlike production of hadrons with local compensation of quantum numbers. In JETSET, particle production is implemented via string fragmentation. Baryons (B) are formed when a diquark pair is contained in the string (see diagram a below), thus resulting in a strong baryon-antibaryon correlation. This correlation can be softened by the "popcorn effect" when an additional meson (M) is produced between the baryon pair as shown in the diagrams b and c below. In contrast, HERWIG describes fragmentation via the formation of clusters and their subsequent decay. Baryons are produced by the isotropic cluster decay into a baryon pair, which can result in stronger correlations than those predicted by JETSET.

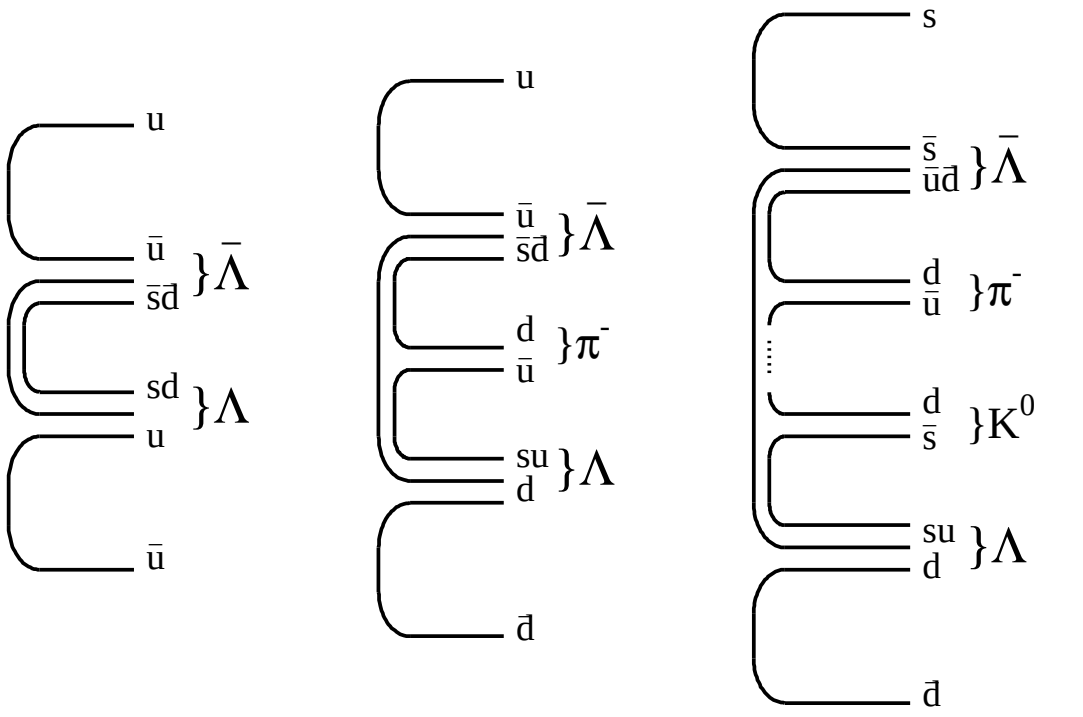

(a) Diquark ($B\bar{B}$) JETSET/MOPS (b) Popcorn ($BM\bar{B}$) JETSET (c) Popcorn ($B(n*M)\bar{B}$) MOPS

Di-lambda production in multihadronic Z^0 decays has been studied over the past years by experiments at PETRA, PEP and LEP [3–7]. These experiments report short-range correlations as observed in the distributions of the rapidities y or rapidity differences $|\Delta y|$ of correlated $\Lambda\bar{\Lambda}$ pairs. The rapidity of a particle is defined as $y = \frac{1}{2}\ln\left(\frac{E+p_\parallel}{E-p_\parallel}\right)$, where E is the energy of the particle and $p_\parallel$ the longitudinal momentum with respect to the thrust axis. Rapidity differences are Lorentz-invariant under boosts along the event axis. These correlations are compared to predictions of JETSET and HERWIG. Satisfactory agreement is found with the

predictions of JETSET when ρ, the "popcorn parameter"[1], is set to the default value, $\rho = 0.5$. However, the tune of other parameters modeling baryon production significantly influences the predictions [8]. HERWIG on the other hand predicts correlations much larger than those experimentally observed.

The full data sample of 4.3 million hadronic Z^0 decays collected with the OPAL detector at LEP in the region of the Z^0 peak is used in this investigation. It supplements the earlier OPAL work [7] by increased statistics and a more robust technique to remove the background contributions from the $\Lambda\bar{\Lambda}$ and $\Lambda\Lambda(\bar{\Lambda}\bar{\Lambda})$ samples in order to obtain a correlated $\Lambda\bar{\Lambda}$ sample which is as clean as possible. The $\Lambda\bar{\Lambda}$ correlations are investigated mainly via rapidity differences. They are compared to the earlier LEP results and to the predictions of JETSET and HERWIG. The predictions of the recent JETSET modification MOPS (MOdified Popcorn Scenarium) [9] are also considered. Correlated $\Lambda\bar{\Lambda}$ pairs are also studied in 2-jet events in which models can be tested with improved sensitivity (compared to the full data sample) when rapidity differences are investigated. Finally, we study correlated $\Lambda\bar{\Lambda}$ pairs within the same and within different jets.

Section 2 gives a short description of the OPAL detector and presents the selection of the Λ events[2] in the total sample and also in 2-jet and 3-jet events, for both experimental and simulated data. In section 3 the separation of the $\Lambda\bar{\Lambda}$ and $\Lambda\Lambda(\bar{\Lambda}\bar{\Lambda})$ samples from the background and the determination of the rates of correlated $\Lambda\bar{\Lambda}$ pairs as a function of the rapidity differences $|\Delta y|$ are discussed. Section 4 contains the measured rates with their errors and a comparison to earlier results as well as the presentation of the differential distributions as a function of $|\Delta y|$ and $\cos\theta^*$, where θ^* is the angle between the thrust axis and the Λ momentum calculated in the rest frame of the di-lambda pair. In section 5 the models are tested using the production rates of Λ pairs as well as the $\cos\theta^*$ and $|\Delta y|$ spectra of correlated $\Lambda\bar{\Lambda}$ pairs. The range of di-lambda correlations is investigated in section 6 by the assignment of the Λ's to the jets. Conclusions are drawn in section 7.

2 Experimental Procedure

2.1 The OPAL Detector

A detailed description of the OPAL detector can be found in Ref. [10]. Of most relevance for the present analysis is the tracking system and the electromagnetic calorimeter. The tracking system consists of a silicon microvertex detector, an inner vertex gas chamber, a large-volume jet chamber and specialized chambers at the outer radius of the jet chamber which improve the measurements in the z direction (z-chambers)[3]. The tracking system covers the region $|\cos\theta| < 0.95$ and is located within a solenoidal magnet coil with an axial field of 0.435 T. The tracking detectors provide momentum measurements of charged particles, and particle identification from measurements of the ionization energy loss, $\mathrm{d}E/\mathrm{d}x$. Electromagnetic energy is measured by a lead-glass calorimeter located outside the magnet coil, which covers $|\cos\theta| < 0.98$.

[1]The value of ρ can be set in JETSET with the parameter PARJ(5): $\rho = \frac{BM\bar{B}}{B\bar{B}+BMB} = \frac{\mathrm{PARJ(5)}}{0.5+\mathrm{PARJ(5)}}$.

[2]For simplicity Λ refers to both Λ and $\bar{\Lambda}$.

[3]The coordinate system is defined so that z is the coordinate parallel to the e^- beam axis, r is the coordinate normal to the beam axis, ϕ is the azimuthal angle around the beam axis, and θ is the polar angle with respect to z.

2.2 Data Samples

The analysis is based on hadronic Z^0 decays collected around the Z^0 peak from 1990 to 1995 (total LEP 1 statistics). The hadronic events were selected with the standard OPAL procedure [11] based on the number and quality of the measured tracks and the electromagnetic clusters and on the amount of visible energy in the event. In addition, events with the thrust axis close to the beam direction were rejected by requiring $|\cos\theta_{\rm thrust}| < 0.9$, where $\theta_{\rm thrust}$ is the polar angle of the thrust axis. With the additional requirement that the jet chamber and the z-chambers were fully operational, a total of 3.895 million hadronic events remained for further analysis, with an efficiency of $(98.4 \pm 0.4)\%$. The remaining background processes, such as $e^+e^- \to \tau^+\tau^-$ and two photon events, were estimated to be at negligible level (0.1% or less).

After the Λ-selection which will be described below, the selection of 2- and 3-jet events was performed. Charged tracks and electromagnetic clusters not associated with any track were grouped into jets using the $k_\perp$ recombination algorithm [12] with a cut value $y_{\rm cut} = 0.005$. In addition to the standard selection criteria, the energy of the clusters and the momenta of the charged tracks had to be less than 60 GeV/c. To improve the quality of the jets it was finally required that there be at least two charged particles per jet (in addition to the possible tracks from Λ decays) and that the minimum energy per jet was 5 GeV. The cuts on the quality of jets were chosen to be this loose to keep the kinematic range as large as possible for comparison with fragmentation models. In total, samples of 1.7 million 2-jet events and 1.4 million 3-jet events were available for further analysis corresponding to 45% and 36%, respectively, of the entire data set.

2.3 Monte Carlo Event Samples

Monte Carlo hadronic events with a full simulation of the OPAL detector [13] and including initial-state photon radiation were used (a) for evaluation of detector acceptance and resolution and (b) for studying the efficiency of the di-lambda reconstruction as a function of the rapidity differences. In total, seven million simulated events were available, of which four million were generated by JETSET 7.4 with fragmentation parameters described in [14], and three million were generated by JETSET 7.3 with fragmentation parameters described in [15]. The two JETSET versions differ in the particle decay tables and heavy meson resonances. There are also some differences in the simulation of baryon production between the two samples. Their small influence on the efficiency correction to the experimental data is accounted for in the systematic errors (see section 4.3).

For comparison with the experimental results, the Monte Carlo models JETSET 7.4 and HERWIG 5.9 [16][4] were used. Both models give a good description of global event shapes and many inclusive particle production rates, but differ in their description of the perturbative phase and their implementation of the hadronization mechanism.

Tracks and clusters are selected in the Monte Carlo events, which include detector simulation, in the same way as for the data, and the resulting four-vectors of particles are referred to as being at the 'detector level'. Alternatively, for testing the model predictions, Monte Carlo samples without initial-state photon radiation nor detector simulation are used, with all charged and

[4]The fragmentation parameters of HERWIG 5.9 were identical to those used in our tuned version of HERWIG 5.8 [16] with the exception of the maximum cluster mass (`CLMAX`) which was set to 3.75 GeV in order to improve the description of the mean charged particle multiplicity in inclusive hadronic Z^0 decays.

neutral particles with mean lifetimes greater than 3×10^{-10} s treated as stable. The four-vectors of the resulting particles are referred to as being at 'generator level'.

2.4 Λ Reconstruction

Neutral strange Λ baryons were reconstructed in their decay channel $\Lambda \rightarrow \pi^-\mathrm{p}$ as described in [17]. Briefly, tracks of opposite charge were paired and regarded as a secondary vertex candidate if the track pair intersection in the plane perpendicular to the beam axis satisfied the criteria of a neutral two-body decay with a decay length of at least 1 cm.

Each candidate track pair was refitted with the constraint that the tracks originated from a common vertex, and background from photon conversions was suppressed. Information from $\mathrm{d}E/\mathrm{d}x$ measurements was used as in [17] to help identify the π and p for further background suppression, primarily due to $\mathrm{K^0_S}\rightarrow \pi^+\pi^-$. Two sets of cuts, called 'method 1' and 'method 2' are described in [17] for Λ identification. For the present analysis, Λ candidates were reconstructed using method 1, which is optimized to have good mass and momentum resolution.

By these means a narrow Λ mass peak above a small background has been obtained. The selection of di-lambda candidates with both invariant masses in the range $1.1057\ \mathrm{GeV}/c^2 < m_{\pi p} < 1.1257\ \mathrm{GeV}/c^2$ (region A in figure 1) retains most of the Λ signal for further analysis.

3 Selection of Correlated Λ-pairs

3.1 Method

Events with more than one Λ candidate that had passed the above selection criteria were considered and all possible pair combinations of the Λ and $\bar{\Lambda}$ baryons within an event were formed. This resulted in pairs of $\Lambda\bar{\Lambda}$, $\Lambda\Lambda$ and $\bar{\Lambda}\bar{\Lambda}$. Combinations were rejected if the pair had a track in common. The remaining pairs are henceforth referred to as Λ-pair candidates.

The three types of baryon pairs can be grouped into two classes: pairs with different baryon numbers $\Lambda\bar{\Lambda}$ and pairs with equal baryon numbers $\Lambda\Lambda(\bar{\Lambda}\bar{\Lambda})$. Only in $\Lambda\bar{\Lambda}$ pairs can the baryon and flavor quantum numbers be compensated by correlated production. $\Lambda\Lambda(\bar{\Lambda}\bar{\Lambda})$ pairs can never be produced in correlation and hence they will occur only in events with more than one baryon-antibaryon pair ($\mathrm{B\bar{B}}$). In such events uncorrelated $\Lambda\bar{\Lambda}$ pairs from different ($\mathrm{B\bar{B}}$) pairs are also possible. The number of uncorrelated $\Lambda\bar{\Lambda}$ pairs corresponds to the number of pairs with same baryon number. Hence, the number of correlated $\Lambda\bar{\Lambda}$ pairs can be derived via

$$N^{\mathrm{corr.}}_{\Lambda\bar{\Lambda}} = N_{\Lambda\bar{\Lambda}} - (N_{\Lambda\Lambda} + N_{\bar{\Lambda}\bar{\Lambda}})\,. \tag{1}$$

At this stage 9479 $\Lambda\bar{\Lambda}$ and 4217 ($\Lambda\Lambda$+$\bar{\Lambda}\bar{\Lambda}$) pair candidates are selected.

3.2 Background Subtraction and Efficiency Correction

Due to the small statistical errors it is necessary to keep systematic uncertainties as low as possible in this analysis. The correct subtraction of non-Λ background from the pairs is therefore

of particular importance. This background consists mainly of other long-lived particles with similar decay topologies (namely $K^0_S \to \pi^+\pi^-$) and random track combinations. An important contribution to the contamination is the so-called correlated background from Λcandidates that have been reconstructed with one false decay track. They are more numerous in pairs with opposite baryon number because the number of $\Lambda\bar{\Lambda}$ pairs is far higher than the number of $\Lambda\Lambda(\bar{\Lambda}\bar{\Lambda})$ pairs. For this reason the background has to be estimated in the two samples separately. Background pairs occur when either one or both Λ-candidates are fake. In the two-dimensional mass plane in figure 1, pairs with one fake Λ form horizontal and vertical bands of background, while pairs with two fake candidates are uniformly distributed in the region above the lower mass bounds.

The background was subtracted using a two-dimensional sideband method. The background in the signal region A was measured from two mass windows (sidebands) of the same size (regions B_1 and B_2) placed in the two bands of background. In this way the background with two fake candidates is counted twice. The latter was determined from region C outside the bands. Hence, the signal is obtained with the subtraction:

$$\text{Signal} = N_{\text{A}} - (N_{\text{B}_1} + N_{\text{B}_2} - N_{\text{C}}) \ .$$

We optimized the position of the sidebands with a MC test investigating the deviations between the background-corrected sample and the true-Λ sample. The stability of this method was tested in the experimental data by shifting the position of the sidebands by one half of the band size from the optimized position. The fluctuations were of the same size as the deviations found in the MC.

Finally the background-corrected $\Lambda\bar{\Lambda}$ and $\Lambda\Lambda(\bar{\Lambda}\bar{\Lambda})$ signal distributions were corrected for detector acceptance and reconstruction efficiency as functions of $|\Delta y|$ and $\cos\theta^*$. The average efficiency in the total hadronic sample was found to be $\approx 2\%$, varying between 1.3% and 2.5% over the $|\Delta y|/\cos\theta^*$ range.

4 Experimental Results

In an earlier OPAL paper [7] based on the 1990 and 1991 data samples we already investigated the production dynamics of baryon-antibaryon pairs. In this section, we present the rates and differential distributions of Λ pairs using the full 1990 to 1995 LEP 1 data in three samples: the entire set of multihadronic events, the 2-jet and the 3-jet events.

4.1 Pair Production Rates

The resulting rates for $\Lambda\bar{\Lambda}$ and $\Lambda\Lambda(\bar{\Lambda}\bar{\Lambda})$ pairs in all hadronic events, determined as sum over all corrected $|\Delta y|$ bins, are given in table 1. The rates for the correlated $\Lambda\bar{\Lambda}$ pairs are derived according to equation (1) from the difference of the opposite and same baryon number pairs. Compared to the results from other LEP experiments and to the previous OPAL publication, good agreement is found.

The di-lambda rates in 2- and 3-jet events are listed in table 2. In 3-jet events, due to the higher color charge of the gluons, the average pair multiplicity is higher.

4.2 Differential Distributions

We studied the correlations in the differential $\Lambda\bar{\Lambda}$ spectra using the observables $|\Delta y|$ and $\cos\theta^*$ as they are particularly sensitive for comparison with Monte Carlo models. The differential distributions are shown in figure 2. The short-range correlations show up as a peak in the region $|\Delta y| \leq 2.0$.

When investigating $|\Delta y|$ distributions, we will restrict ourselves to 2-jet events. This is due to the fact that in 3-jet events many particle momenta have large angles to the thrust axis, resulting in smaller longitudinal momenta and smaller rapidity differences, independent of correlations. As a result the $|\Delta y|$ distribution is broader and less steep in 2-jet events than in the 3-jet or the total sample (see figure 2a). Consequently, also the range of variations is larger in 2-jet events and yields a higher sensitivity in the comparison with model predictions.

4.3 Systematic Errors

The systematic error is found to be largely independent of $|\Delta y|$ and $\cos\theta^*$, and in the subsequent discussion of the differential distributions of the correlated pairs, only normalized distributions are considered. These are largely insensitive to effects of systematic uncertainties. Consequently, the systmatic errors discussed below are mainly relevant for the total rates.

For the determination of the experimental uncertainties we considered the following sources of systematic effects:

- Uncertainties due to the subtraction of background via the sidebands. These were estimated using simulated events by applying the analysis to the fully detector simulated MC and comparing the rate from the background corrected sample to the true number.
- Efficiency uncertainties. These were estimated from the difference of the results when the efficiency correction was done using both JETSET versions 7.3 and 7.4 samples in combination and using them separately.
- The statistical error of the efficiency due to the limited sample size of the simulated events at detector level.
- Uncertainties in the modelling of the cut variables used for the Λ selection. This error is taken from a former analysis [17] where it was determined very precisely for single Λ's. The error given there is doubled for the Λ pairs in the present analysis.

These effects contribute to the total systematic error as shown in table 3, where the relative systematic errors from the different sources are compared to the total systematic as well as to the statistical error. Statistical and total systematic errors contribute about equally.

5 Comparison with Fragmentation Models

We start the discussion with the numbers and distributions of the models with OPAL default tunes that optimize the general performance of the models and the agreement with the measured single particle rates.

5.1 Pair Production Rates

We investigate the di-lambda rates first in the total hadronic data sample comparing the measured rates to the predictions of the models JETSET 7.4, MOPS and HERWIG 5.9 (see table 1). None of the models gives a perfect description of the data but HERWIG clearly exhibits the largest disagreement.

The comparison of the di-lambda rates in 2- and 3-jet events is given in table 2. The higher multiplicity in 3-jet events compared to 2-jet events is qualitatively well described by all three models. However, only JETSET yields a prediction compatible with the measured numbers. In the 2-jet event sample the agreement is excellent. In the 3-jet sample all the measured rates exceed the JETSET predictions. This can be compared to the observation that Λ rates in gluon jets are too low in JETSET [18] .

5.2 Differential Distributions

To further investigate the nature of the $\Lambda\bar{\Lambda}$ correlations we compare the differential distributions of correlated $\Lambda\bar{\Lambda}$ pairs with the predictions of the various models. We use the variables $\cos\theta^*$ and $|\Delta y|$ and test their sensitivity to distinguish between the different fragmentation models and baryon production mechanisms. All distributions are of the type $\frac{1}{N}\frac{dN}{d(|\Delta y|)}$, N being the total number of entries. This has the advantage that they are independent of the total rates and that the systematic errors mostly cancel out, since they are nearly independent of both $|\Delta y|$ and $\cos\theta^*$.

The angle θ^* is particularly suited to distinguish between string and cluster fragmentation. The mostly isotropic cluster decay (HERWIG) results in a relatively flat $\cos\theta^*$ distribution whereas string fragmentation produces the correlated $\Lambda\bar{\Lambda}$ system predominantly close to the thrust axis, i.e., with $\cos\theta^* \approx 1$. These predictions are compared to the measurement in figure 3. The data show a distribution that is strongly peaked towards $\cos\theta^* = 1$ and therefore clearly rule out the HERWIG cluster model. The predictions of MOPS agree somewhat better with the experimental distribution but they also fail to model the forward peak correctly. Only JETSET yields a good description of the data.

On the other hand, especially in 2-jet events, the rapidity difference $|\Delta y|$ is more sensitive to show differences in the strength of the correlations. The experimental data and model predictions are compared in figure 4. Again JETSET gives the best, albeit not completely satisfactory, description of the measured distribution. HERWIG generates correlations which are far too strong . The MOPS model with its built-in facility to allow for several "popcorn mesons" should yield weaker correlations than JETSET; however, in contrast to this naive expectation it produces a narrower $|\Delta y|$ distribution, i.e. stronger correlations. We see the following possible reasons for this: first of all, and different from JETSET, a new kinematic property is built into MOPS: the low-Γ-suppression [9]. This suppresses popcorn fluctuations at early times in the color field, resulting in very strong correlations. Secondly, it appears that the strength of the correlations is influenced more by the rate of baryon production via the popcorn mechanism than by the actual number of intermediate mesons produced. As JETSET and MOPS are tuned to show the same mean number of popcorn mesons instead of popcorn systems, MOPS has fewer popcorn systems and therefore stronger correlations.

5.3 Tuning of Models

In an earlier OPAL analysis of strange baryons [8] it was observed that the agreement between experimental data and JETSET predictions can be improved by adjusting some of the diquark parameters: improving the predicted shape of the $|\Delta y|$ distribution was possible by varying the popcorn parameter, ρ=PARJ(5), that influences the frequency of popcorn production and hence the correlation strength. It was found that ρ acts on both the shape of the rapidity spectrum and the production rates. Two other parameters were used to correct for this change of predicted multiplicities: the ratio of the strange to non-strange diquarks over strange to non-strange quarks, (us:ud/s:d) = PARJ(3), and the ratio of spin-1 to spin-0 diquarks, $(1/3 \cdot [\mathrm{qq}]_1/[\mathrm{qq}]_0)$=PARJ(4). These last parameters affect mainly the rates and leave the spectra nearly unmodified. When attempting to improve the predictions of the MOPS model in the same manner, the most direct correspondence to ρ in JETSET is the MOPS parameter PARJ(8)=β(u), the transverse mass of an intermediate u-quark. The higher the transverse mass of the intermediate system (with several quark pairs possible), the lower the probability to produce this popcorn system and the stronger the correlations. Therefore, in both JETSET and MOPS we tried first to improve the agreement with the data distributions by tuning the parameters that influence the correlation strength (figure 5 for JETSET.) In JETSET, the popcorn probability ρ was varied from 0%-90%, while in MOPS the transverse mass of a u-quark, β(u)=PARJ(8), was altered between 0.2 and 1.0 GeV^{-1}. All other parameters remained at the OPAL default values. As can be seen from table 5, for the ρ parameter, these variations affect not only the shape of the $|\Delta y|$ distribution but also the di-lambda rates, as expected.

The predictions with the different popcorn parameter values in JETSET are compared to the data in figure 5a. Only the results from parameter settings above the default value of $\rho = 0.5$ are shown, since lower values give a poorer agreement with the data. The best agreement is found in the range $0.6 < \rho < 0.8$. Popcorn values within this range also yield good agreement between data and predictions for the $\cos\theta^*$ distribution. However, when the influence of the popcorn parameter on the predicted di-lambda rates is also considered (table 5) use has to be made of the other two JETSET parameters that affect the strange baryon production in order to tune the rates back to values corresponding to the measurement. It can be seen from table 5 and figure 5b that such a tune clearly produces a better agreement with the rates (also for single particle production) while it does not change the spectra of rapidity differences significantly. Using the results of other OPAL analyses, it can also be seen that the tune does not change the strange meson (K^0_S) rate, nor does it affect the non-strange baryon (p) rate significantly. The known problems [8] in modeling the decuplet baryon rates are also seen here. No further attempt has been made to globally optimize the parameter set, however.

The tune of parameter PARJ(8) in MOPS did not result in an improvement. Although the value of the parameter was varied in a comparatively wide range, the effect on the $|\Delta y|$ distribution was almost imperceptible. PARJ(8) clearly is not suited to adjust the MOPS model to the data. Therefore, we tested another parameter of the model using the relative difference between the fragmentation function $f(z)$ for baryons and mesons, the parameter PARJ(45). Again, the variation did not notably change the shape of the distribution. This relatively poor performance of the MOPS Monte Carlo in describing the $|\Delta y|$ dependent $\Lambda\bar{\Lambda}$ correlations seems to be connected to the known shortcomings of the model in describing $p_\perp$-related distributions [9].

6 Di-lambdas in Jets

After studying the strength of $\Lambda\bar{\Lambda}$ correlations in the $|\Delta y|$ spectra, we will now present results on the range of the correlations by assigning both partners from a correlated pair to the reconstructed jets in an event. For short-range correlations both partners are expected within the same jet whereas long-range correlations (which can be obtained by the production of baryons from the primary quarks) should result in an assignment to different jets. We use the following two classifications for the assignment study: both partners within the same jet, and each partner in a different jet.

Due to the fact that it is impossible to map 2-jet events at detector level to 2-jet events at generator level, we do not attempt to apply efficiency corrections but compare our uncorrected results with the JETSET predictions at detector level. We count the number of $\Lambda\bar{\Lambda}$ and $\Lambda\Lambda(\bar{\Lambda}\bar{\Lambda})$ pairs in each sample and obtain the number of correlated pairs again from the relation $N_{\Lambda\bar{\Lambda}}^{\text{correlated}} = N_{\Lambda\bar{\Lambda}} - (N_{\Lambda\Lambda} + N_{\bar{\Lambda}\bar{\Lambda}})$. The amount of background in like- and unlike-sign pairs approximately cancels out in this subtraction as long as the contribution from the correlated background (see section 3.2) can be neglected. The numbers of pairs obtained from the same jet and from different jets are listed in table 4 for both 2- and 3-jet events. The major part of the correlated pairs is reconstructed within the same jet (about 96% in 2-jet events, 81% in 3-jet events) whereas only a very small fraction is found in different jets. These experimental numbers are in excellent agreement with the JETSET predictions at detector level and support the assumption of short-range compensation of baryon number and strangeness in the fragmentation process.

7 Summary

$\Lambda\bar{\Lambda}$ correlations have been studied in 4.3 million multihadronic Z^0 decays, with the correlated sample obtained from the difference: $\Lambda\bar{\Lambda}_{\text{corr}}$=$\Lambda\bar{\Lambda}$–($\Lambda\Lambda$+$\bar{\Lambda}\bar{\Lambda}$). The analysis has been performed in terms of $\cos\theta^*$ and rapidity differences $|\Delta y|$. As the rapidity is defined with respect to the event (thrust) axis, the sensitivity of the analysis is seen to be higher in 2-jet events. Therefore three data samples have been analyzed: the entire hadronic event sample, 2-jet events (45%), and 3-jet events (36%). The experimental findings have been used to study the baryon production mechanism implemented in various phenomenological fragmentation models.

The following results have been obtained:

- In the full data set, the measured production rates of $\Lambda\bar{\Lambda}$, $\Lambda\Lambda(\bar{\Lambda}\bar{\Lambda})$ and, consequently, $\Lambda\bar{\Lambda}_{\text{corr}}$ are in good agreement with a previous OPAL measurement and results from ALEPH and DELPHI, but show significantly smaller errors.

- The $\cos\theta^*$ distribution of correlated Λ-pairs is well suited to distinguish between isotropic cluster and non-isotropic string decay, and clearly favours the latter, implemented in JETSET. The predictions of the isotropic cluster model HERWIG are ruled out by the data: they do not describe the features of correlated $\Lambda\bar{\Lambda}$ production.

- The rapidity difference $|\Delta y|$ is used to study the strength of correlated di-lambda production. The measured distribution exhibits strong local correlations.

- Satisfactory reproduction of the experimental results is obtained with the predictions of the string fragmentation model JETSET. Improved agreement can be found by tuning some of the default parameters used by OPAL. After adjusting the popcorn parameter, to improve the description of the $|\Delta y|$ spectrum, other parameters, fixing the fraction of diquarks with strangeness and spin1, have to be modified to readjust the predicted rates to the experimental ones. This procedure does not affect the previously optimized $|\Delta y|$ distribution. The HERWIG model cannot describe the measured $|\Delta y|$ spectra, and the predictions of MOPS, a recently published modification of the JETSET model, also fail to reproduce the experimental data, even after some parameter tuning.

- In the 2-jet and 3-jet event samples it is found that correlated $\Lambda\bar{\Lambda}$ pairs are produced predominantly within the same jet, supporting the assumption of a short-range compensation of quantum numbers. Again, the JETSET predictions are in good agreement with the experimental results.

In conclusion, the analysis of correlated di-lambda pairs proves to be a very effective tool to test fragmentation models. JETSET is the only candidate model studied, describing the data successfully.

Acknowledgements:

We are grateful to P. Eden for various interesting discussions about the performance of the MOPS model and for his interest in our results.
We particularly wish to thank the SL Division for the efficient operation of the LEP accelerator at all energies and for their continuing close cooperation with our experimental group. We thank our colleagues from CEA, DAPNIA/SPP, CE-Saclay for their efforts over the years on the time-of-flight and trigger systems which we continue to use. In addition to the support staff at our own institutions we are pleased to acknowledge the
Department of Energy, USA,
National Science Foundation, USA,
Particle Physics and Astronomy Research Council, UK,
Natural Sciences and Engineering Research Council, Canada,
Israel Science Foundation, administered by the Israel Academy of Science and Humanities,
Minerva Gesellschaft,
Benoziyo Center for High Energy Physics,
Japanese Ministry of Education, Science and Culture (the Monbusho) and a grant under the Monbusho International Science Research Program,
German Israeli Bi-national Science Foundation (GIF),
Bundesministerium für Bildung, Wissenschaft, Forschung und Technologie, Germany,
National Research Council of Canada,
Research Corporation, USA,
Hungarian Foundation for Scientific Research, OTKA T-016660, T023793 and OTKA F-023259.

References

[1] T. Sjöstrand, Comp. Phys. Comm. **82** (1994) 74.

[2] G. Marchesini et al., Comp. Phys. Comm. **67** (1992) 465.

[3] JADE Collaboration, W. Bartel et al., Phys. Lett. **B104** (1985) 325;
TASSO Collaboration, M. Althoff et al., Z. Phys. **C27** (1985) 27.

[4] TPC Collaboration, H. Aihira et al., Phys. Rev. Lett. **55** (1985) 1047;
MARK2 Collaboration, C. de la Vaissiere et al., Phys. Rev. Lett. **54** 2071.

[5] ALEPH Collaboration, R. Barate et al., Phys. Rept. **294** (1998) 1.

[6] A. Bohrer, Phys. Rept. **291** (1997) 107.

[7] OPAL Collaboration, P. Acton et al., Phys. Lett. **B305** (1993) 415.

[8] OPAL Collaboration, P. Acton et al., Phys. Lett **B291** (1992) 503.

[9] P. Eden and G. Gustafson, Z. Phys. **C75** (1997) 41.

[10] OPAL Collaboration, K. Ahmet et al., Nucl. Instr. and Meth. **A305** (1991) 275;
P. Allport et al., Nucl. Instr. and Meth. **A324** (1993) 34;
P. Allport et al., Nucl. Instr. and Meth. **A346** (1994) 476.

[11] OPAL Collaboration, G. Alexander et al., Z. Phys. **C52** (1991) 175.

[12] S. Catani et al., Phys. Lett. **B269** (1991) 432;
N. Brown and W.J. Stirling, Z. Phys. **C53** (1992) 629.

[13] OPAL Collaboration, J. Allison et al., Nucl. Instr. and Meth. **A317** (1992) 47.

[14] OPAL Collaboration, G. Alexander et al., Z. Phys. **C69** (1996) 543.

[15] OPAL Collaboration, P. Acton et al., Z. Phys. **C58** (1993) 387.

[16] OPAL Collaboration, G. Alexander et al., Z. Phys. **C71** (1996) 191.

[17] OPAL Collaboration, G. Alexander et al., Z. Phys. **C73** (1997) 569.

[18] OPAL Collaboration, K. Ackerstaff et al., "Production of K^0_S and Λ in Quark and Gluon Jets from Z^0 decay", CERN-EP/98-058, submitted to Eur. Phys. J.

[19] OPAL Collaboration, R. Ackers et al., Z. Phys. **C67** (1995) 389.

[20] OPAL Collaboration, R. Ackers et al., Z. Phys. **C63** (1994) 181.

[21] OPAL Collaboration, G. Alexander et al., Z. Phys. **C73** (1997) 587.

[22] OPAL Collaboration, G. Alexander et al., Phys. Lett. **B358** (1995) 162.

Tables

	N_{pairs}/Hadronic Event [$\times 10^{-2}$]		
	$\Lambda\bar{\Lambda}$	$\Lambda\Lambda(\bar{\Lambda}\bar{\Lambda})$	$\Lambda\bar{\Lambda}_{\mathrm{corr}}$
This Analysis	$8.95 \pm 0.15 \pm 0.31$	$2.83 \pm 0.11 \pm 0.17$	$6.12 \pm 0.19 \pm 0.28$
OPAL [7]	$8.26 \pm 0.42 \pm 0.79$	$2.05 \pm 0.39 \pm 0.28$	$6.21 \pm 0.54 \pm 0.84$
ALEPH [5]	9.3 ± 0.9	2.8 ± 0.3	6.5 ± 1.0
DELPHI [6]	9.0 ± 0.9	1.8 ± 0.6	7.2 ± 1.1
JETSET 7.4	7.75	2.24	5.51
MOPS	10.57	2.63	7.94
HERWIG 5.9	15.09	3.06	12.03

Table 1: Comparison of average Λ pair multiplicities from this analysis with those from a previous OPAL analysis, with the results from other LEP experiments and with model predictions. The statistical error is given first, the systematic error second. For ALEPH and DELPHI only the total error is available.

	$\Lambda\bar{\Lambda}$	$\Lambda\Lambda(\bar{\Lambda}\bar{\Lambda})$	$\Lambda\bar{\Lambda}_{\mathrm{corr}}$
	N_{pairs}/2-Jet Event [$\times 10^{-2}$]		
OPAL data	$5.99 \pm 0.21 \pm 0.30$	$1.44 \pm 0.14 \pm 0.15$	$4.55 \pm 0.25 \pm 0.31$
JETSET 7.4	6.14	1.45	4.69
MOPS	8.34	1.68	6.66
HERWIG 5.9	13.16	2.45	10.71
	N_{pairs}/3-Jet Event [$\times 10^{-2}$]		
OPAL data	$9.55 \pm 0.24 \pm 0.41$	$2.98 \pm 0.18 \pm 0.22$	$6.67 \pm 0.30 \pm 0.32$
JETSET 7.4	8.70	2.66	6.04
MOPS	11.92	3.17	8.75
HERWIG 5.9	16.11	3.31	12.80

Table 2: Average multiplicity of Λ pairs in 2- and 3-jet events compared to model predictions. The statistical error is given first, the systematic error second.

Source of Error	Effect on the $\Lambda\bar{\Lambda}_{\rm corr}$ Rate		
	All Hadr.	2-Jets	3-Jets
Background Systematics	0.9%	2.8%	0.9%
JETSET 7.3/7.4 Mixing	2.3%	3.5%	1.1%
Monte Carlo Statistics	2.3%	4.3%	3.5%
Cut Simulation	3.0%	3.0%	3.0%
Total Syst. Error	4.5%	6.8%	4.8%
Stat. Error	3.1%	5.5%	4.5%

Table 3: Relative errors in measuring the multiplicity of correlated Λ pairs in the three event samples.

Assignment	$\Lambda\bar{\Lambda}$	$\Lambda\Lambda(\bar{\Lambda}\bar{\Lambda})$	$\Lambda\bar{\Lambda}_{\rm corr}$	Fraction of $\Lambda\bar{\Lambda}_{\rm corr}$	
				OPAL data	JETSET det. level
2-Jet Events					
Same Jet	1994	469	1525	$(95.6 \pm 2.3)\%$	$(95.8 \pm 1.8)\%$
Different Jets	719	649	70	$(4.4 \pm 2.3)\%$	$(4.2 \pm 1.8)\%$
3-Jet Events					
Same Jet	2088	409	1679	$(80.6 \pm 1.8)\%$	$(80.6 \pm 1.4)\%$
Different Jets	1174	769	405	$(19.4 \pm 1.8)\%$	$(19.4 \pm 1.4)\%$

Table 4: Assignment of Λ pairs to the reconstructed jets in 2-jet and 3-jet events, compared to the predictions of JETSET 7.4. The errors are statistical only.

	Jetset 7.4			Data
ρ	0.5*	0.7	0.7	
PARJ(3)	0.45*	0.45*	0.60	
PARJ(4)	0.025*	0.025*	0.010	
Di-lambda Pairs in the Total Hadronic Sample				
$\Lambda\bar{\Lambda}$	0.0775	0.0668	0.0859	0.0895 ± 0.0034
$\Lambda\Lambda(\bar{\Lambda}\bar{\Lambda})$	0.0224	0.0187	0.0256	0.0283 ± 0.0020
$\Lambda\bar{\Lambda}_{\rm corr}$	0.0551	0.0481	0.0603	0.0612 ± 0.0034
Di-lambda Pairs in 2-Jet Events				
$\Lambda\bar{\Lambda}$	0.0614	0.0518	0.0677	0.0599 ± 0.0037
$\Lambda\Lambda(\bar{\Lambda}\bar{\Lambda})$	0.0145	0.0119	0.0164	0.0144 ± 0.0021
$\Lambda\bar{\Lambda}_{\rm corr}$	0.0469	0.0399	0.0513	0.0455 ± 0.0040
Particle	Multiplicities			
K^0	2.02	2.03	2.02	1.99 ± 0.04
proton	0.93	0.89	0.92	0.92 ± 0.11
Λ	0.338	0.316	0.361	0.374 ± 0.010
Σ^+	0.075	0.067	0.087	0.099 ± 0.015
Σ^0	0.073	0.065	0.086	0.071 ± 0.018
Σ^-	0.068	0.059	0.080	0.083 ± 0.011
Ξ^-	0.0278	0.0241	0.0341	0.0259 ± 0.0011
Δ^{++}	0.10	0.12	0.08	0.22 ± 0.06
$\Sigma(1385)^{\pm}$	0.0457	0.0546	0.0393	0.0479 ± 0.0044
$\Xi(1530)^0$	0.0036	0.0040	0.0035	0.0068 ± 0.0007
Ω^-	0.0006	0.0006	0.0006	0.0018 ± 0.0004

Table 5: Comparison of inclusive di-lambda yields with Jetset Monte Carlo predictions using the Opal default tune (second column), a tune to obtain agreement with the measured $|\Delta y|$ spectra (third column) and a tune to obtain simultaneous agreement in distributions and rates (fourth column). The measured values with total errors are given in the fifth column. The single particle inclusive rates are given for comparison: the experimental numbers for K^0_S, protons, Σ and Δ^{++} baryons are taken from [19], [20], [21], [22], respectively; the remaining numbers are from [17]. The parameters used for the tune are described in the text. Parameter default values are marked with a star.

Figures

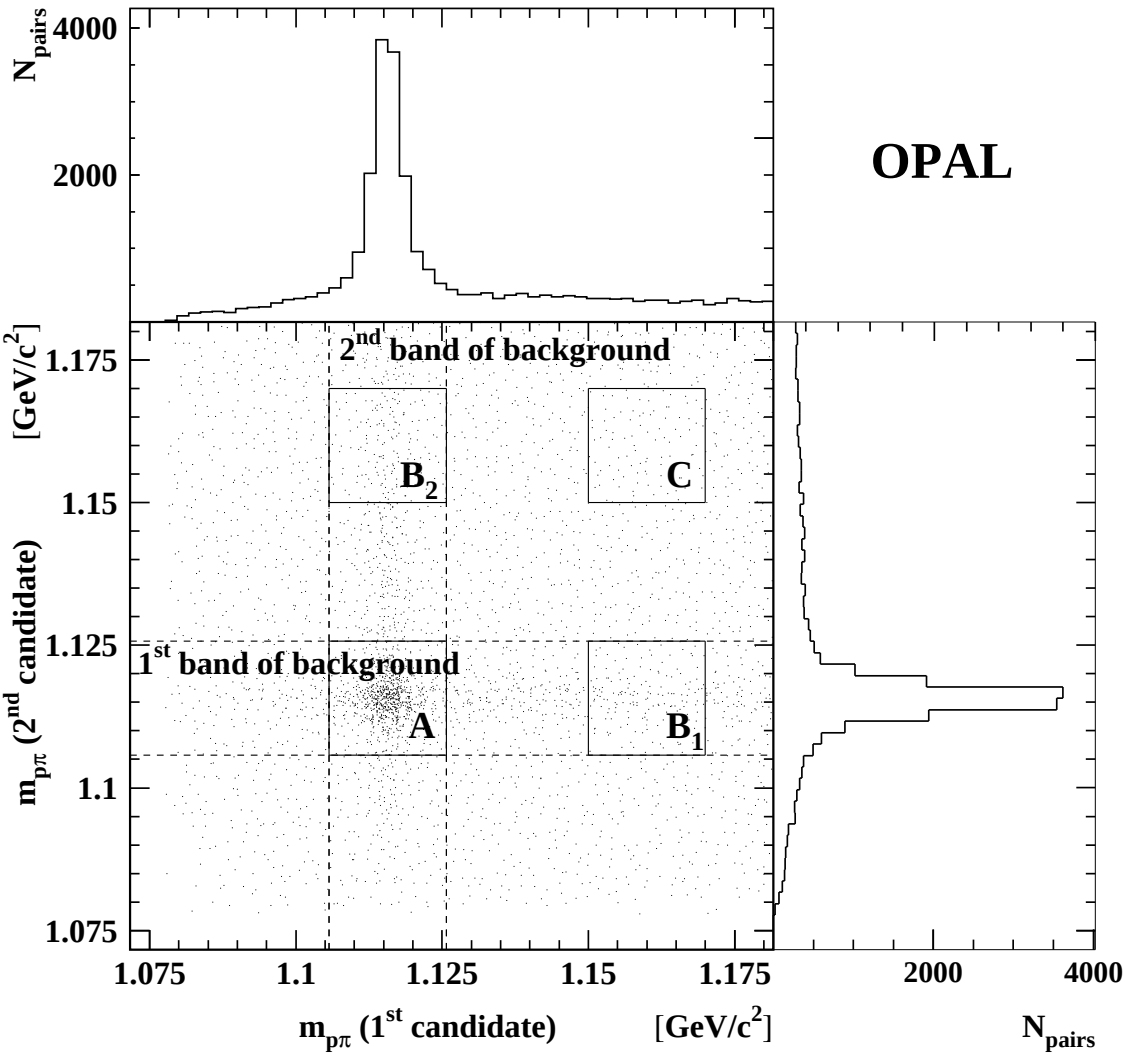

.

Figure 1: Two-dimensional mass distribution of $\Lambda\bar{\Lambda}$ candidates and projections onto the mass axes. The background forms a horizontal and a vertical band from pairs with one fake Λ above a uniform background from two non-Λ candidates. The signal peak at the Λ mass of 1.116 GeV/c^2 is clearly visible.

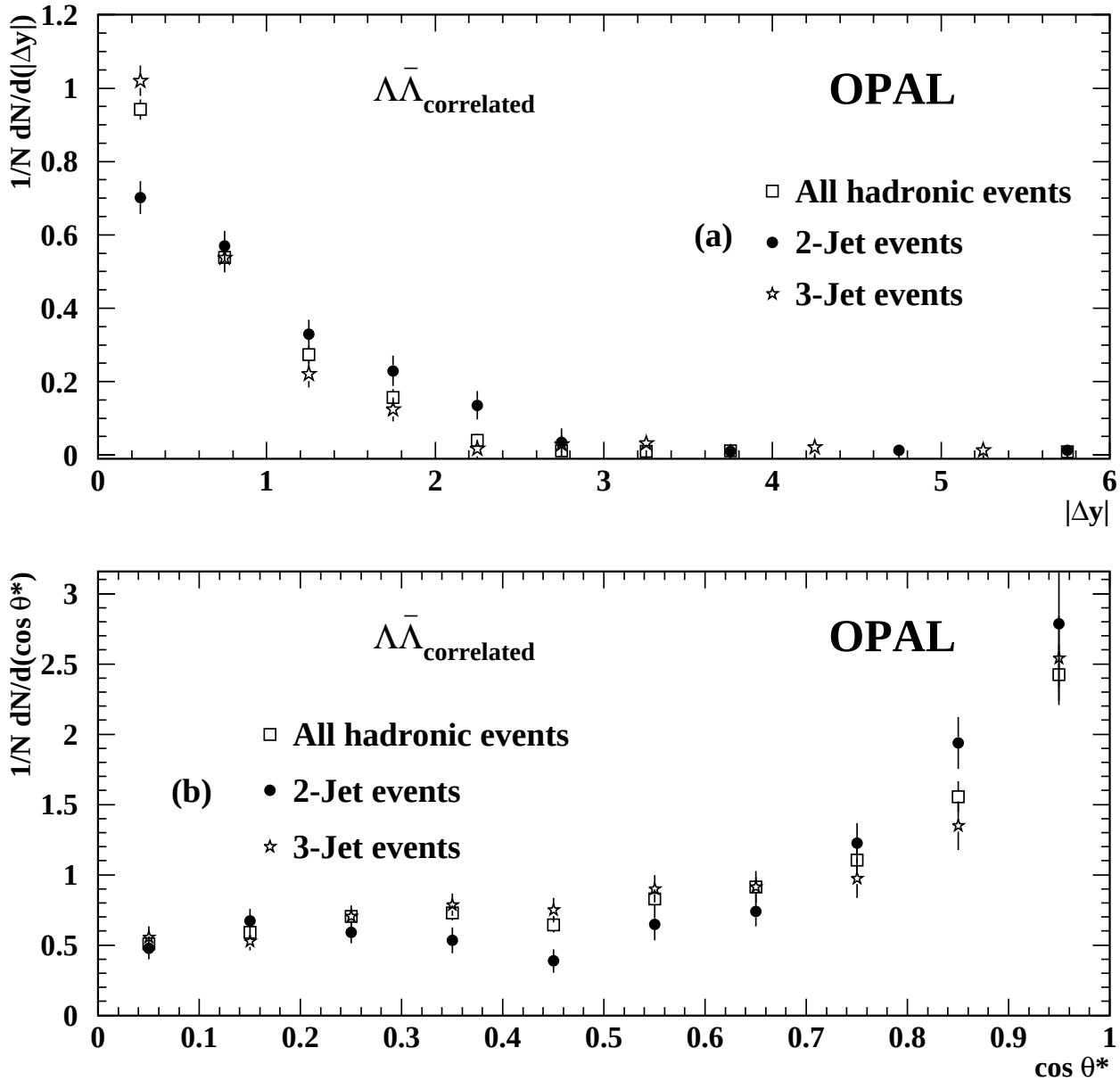

Figure 2: Comparison of the shape of differential distributions in all hadronic events and in 2-/3-jet events for the $|\Delta y|$ distribution in (a) and the $\cos\theta^*$ distribution in (b). The errors shown are purely statistical, the influence of the systematic errors is negligible.

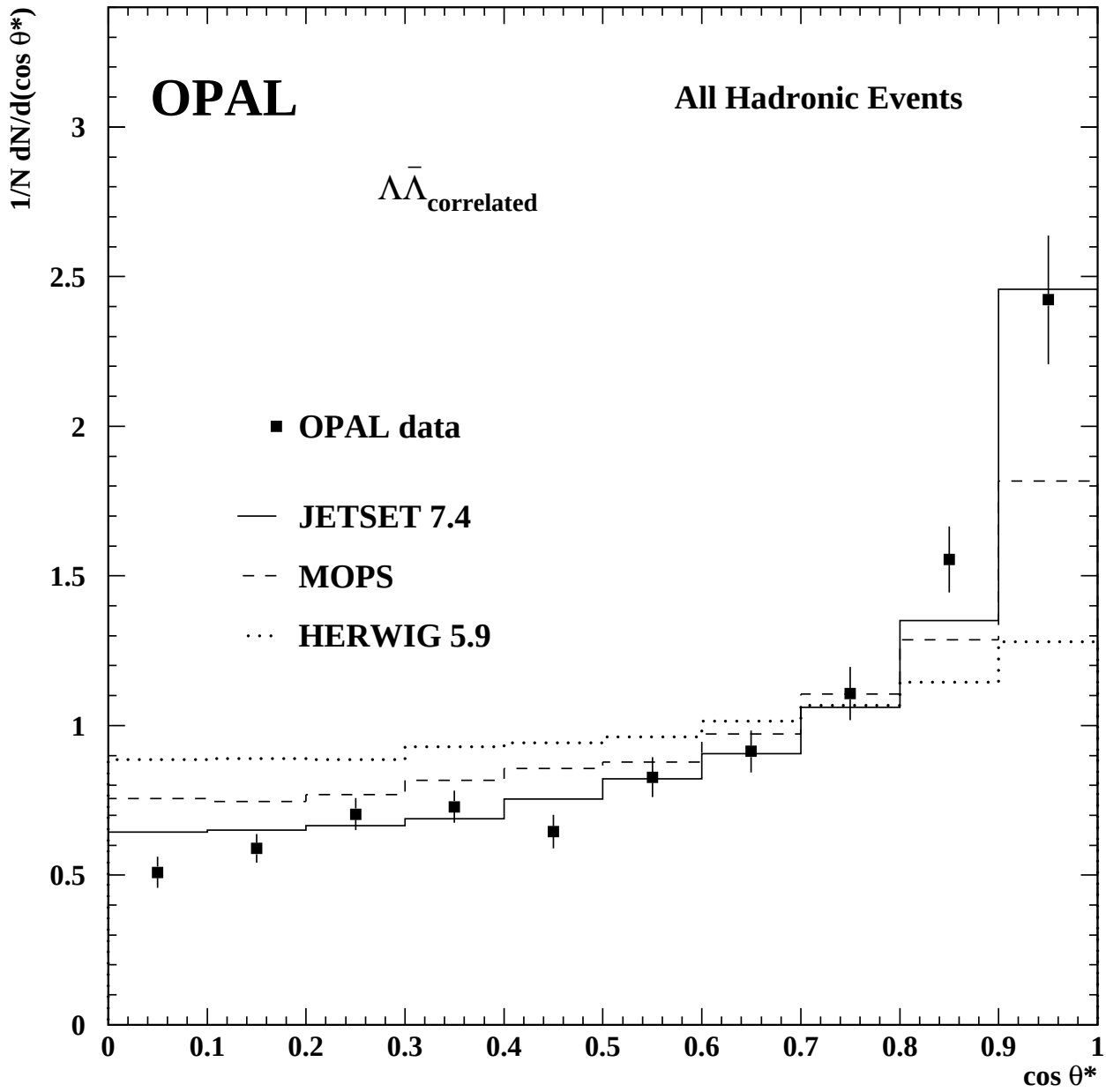

Figure 3: Comparison of the measured distribution of the angle θ^* for correlated $\Lambda\bar{\Lambda}$ pairs in all hadronic events with the predictions from the various models. The errors shown are purely statistical, the influence of the systematic errors is negligible.

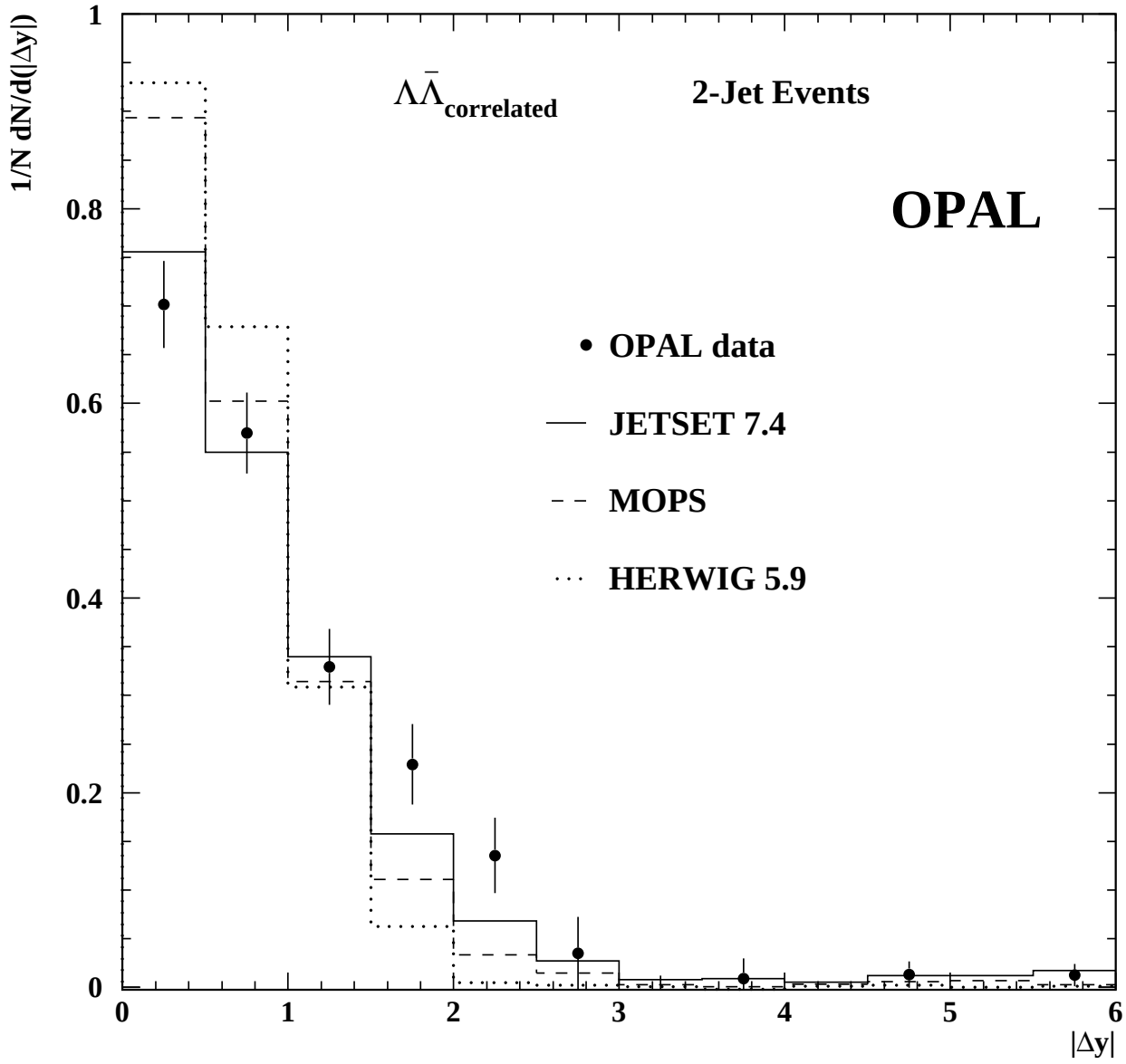

Figure 4: Comparison of the rapidity difference distribution of correlated $\Lambda\bar{\Lambda}$ pairs from the 2-jet events with the model predictions.The errors shown are purely statistical, the influence of the systematic errors is negligible.

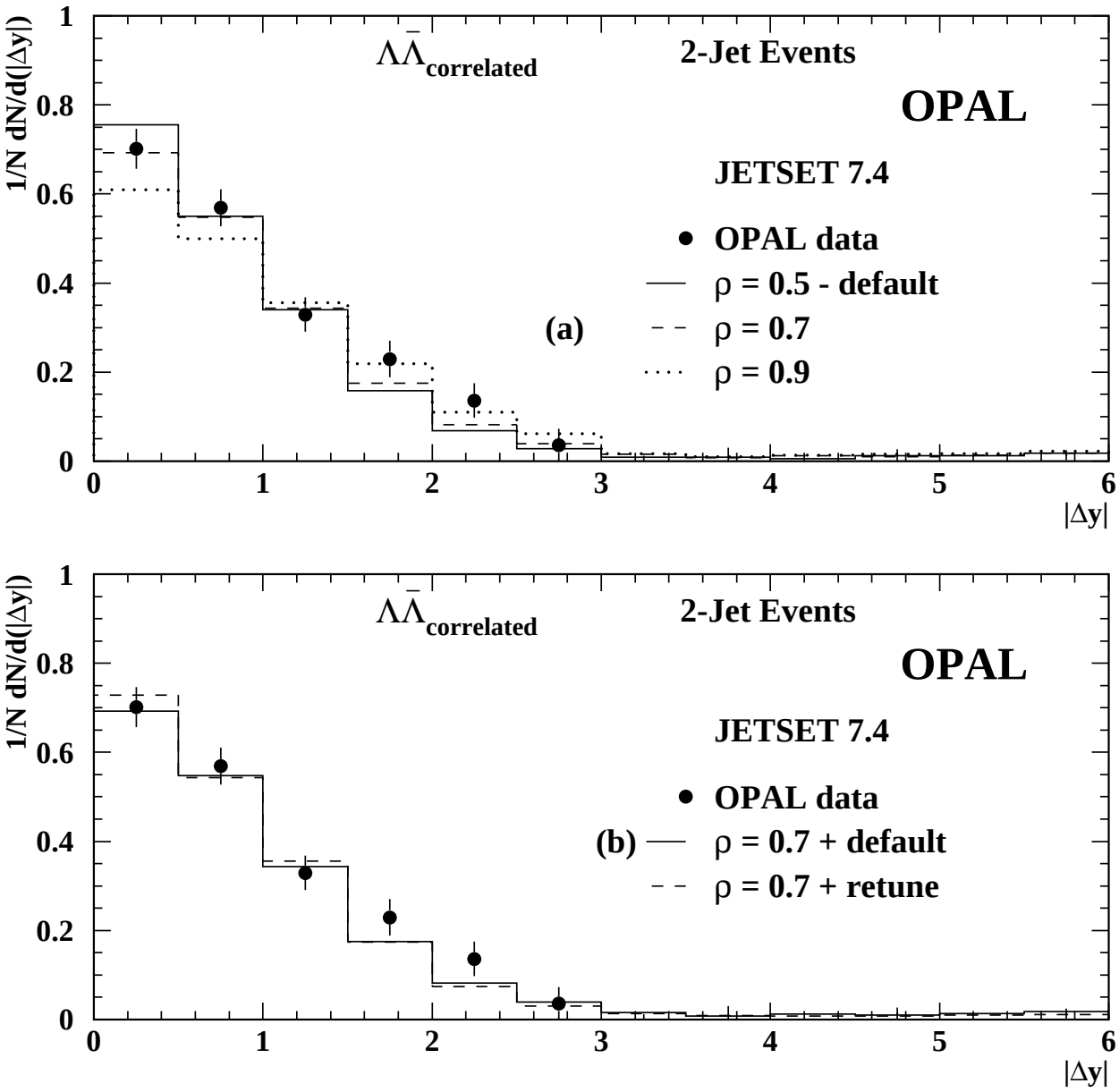

Figure 5: Comparison of the measured rapidity difference distribution of correlated $\Lambda\bar{\Lambda}$ pairs in 2-jet events with the JETSET predictions. (a) Different values of the popcorn parameter (while the other parameters remain at their default values) (b) The best popcorn value (0.7) with and without a retune of PARJ(3,4). The errors shown are purely statistical, the influence of the systematic errors is negligible.